17th Brazilian Congress of Thermal Sciences and Engineering
November 25th-28th, 2018, Águas de Lindóia, SP, Brazil

ENCIT-2018-0096
NUMERICAL STUDY OF COUPLED NATURAL CONVECTION, CONDUCTION AND RADIATION HEAT TRANSFER FOR A TROMBE WALL CONFIGURATION

Taynara Geysa Silva do Lago
Kamal A. R. Ismail
State University of Campinas (UNICAMP) - Faculty of Mechanical Engineering, Department of Energy, 13083-860, Campinas, São Paulo, Brazil
taynaragsl@fem.unicamp.br, kamal@fem.unicamp.br

Abstract. *This study presents the conjugate heat transfer problem in an enclosure heated on one vertical wall and cooled at the other vertical wall for laminar regime. The enclosure has a conducting solid body and the fluid in the enclosure is air. The model is based on the steady state equations of conservation of mass, momentum and energy. Boussinesq approach is used to approximate buoyancy term. The discretization of the conservative equations is done using the finite volume method. A radiation model has been included in the analysis to study the effect of surface radiation on the heat transfer characteristics of the cavity. The coupling of pressure and velocity field is performed through the SIMPLE algorithm. The effect of the conducting body is investigated through streamlines and isotherms for different internal solid sizes, thermal conductivity ratios between solid and fluid varying from 1 to 100 and radiation emissivities for all surfaces from 0 to 1. The results are presented in terms of temperature and velocity distributions in various parts of the system. Results show that radiation is the dominant mode of heat transfer.*

Keywords: *Natural convection, Radiation heat transfer, Cavity, Trombe wall, Passive comfort*

1. INTRODUCTION

Trombe wall is an indirect gain passive solar system which was designed and patented with the purpose of supplying heat and ventilation in buildings using solar radiation. Since then, Trombe wall has been the subject of several studies aiming to improve its thermal performance. The wall absorbs solar radiation and transmits part of it into the dwelling by natural convection through the solar chimney formed by the glazing on one side and the wall on the other. The air circulates through the vents at the bottom and top of the wall into the adjacent room. The natural convection is then controlled by these vents. The various parameters are: Rayleigh number (from 10^3 to 10^6), dimensionless conductivity of bounding wall (from 0 to 100), dimensionless wall thickness (from 0 to 0.6) and dimensionless wall length (0.5 to 1). In the literature, there are theoretical studies that have predicted the behavior of the Trombe wall system considering a thermal network approach while others have used CFD. The present study handles the conjugate heat transfer problem in a square cavity heated on one wall and cooled at the other parallel wall having an internal conducting solid body.

Natural convection in cavities is one of the classic problems of heat transfer having an extensive number of numerical and experimental approaches since the second half of the 20th century. The cavity configurations found in the literature are usually square or rectangular, combining fully or partially heated/cooled walls under constant temperature or heat flow. Natural convection of fluid media in enclosures has received considerable attention largely due to a wide variety of applications including heating and cooling of rooms, cooling of electronic equipments, solar collector technology, energy storage, etc. The problem of natural convection in an enclosure has been extensively studied in literature for various boundary conditions. Comprehensive reviews of natural convection were documented by Vahl Davis and Jones (1983).

Kim and Viskanta (1984) numerically studied the effects of wall conduction and radiation in a two-dimensional rectangular enclosure and determined that these effects reduced natural convection heat transfer. Balaji and Venkateshan (1993) and Akiyama and Chong (1997) studied the effect of surface radiation with free convection in a square cavity

House *et al.* (1990) analyzed the effect of the size and thermal conductivity of a single solid body positioned in the center of an enclosure heated and cooled from its sides. The heat transfer in the enclosure is governed by Rayleigh and Prandtl numbers, the size of the body and its thermal conductivity.

Yedder and Bilgen (1991) studied thermal performance of classical Trombe wall solar collector system. They assumed that the flow is laminar and two-dimensional, the glazing is isothermal and the solar heat absorbed by the wall is transferred to the air in the channel with a constant flux by natural convection and to the adjacent room by conduction and then by convection. They used square cavity, rectangular cavity with aspect ratios of 5.

Mezrhab *et al.* (2006) described a numerical study of the radiation-natural convection interactions in a differentially heated cavity with an internal body. A specifically developed numerical model, based on the finite-volume method, is

used for the solutions of the governing differential equations. The SIMPLER algorithm for the pressure–velocity coupling is adopted. Air is considered transparent to the radiation

Hernandez *et al*. (2016) investigated a room with a Trombe wall system. The simulations were done with an internal code based on the Finite Volume Method. It has been found that the losses of thermal energy through the semitransparent wall are about 60% of the solar radiation incident on the system. Despite thermal losses, the system gets enough energy to keep the air inside the room with a temperature above 35°C. For cities, Huitzilac and Toluca, during the coldest day, the maximum stored energy is about 109 MJ during the day. The hottest is about 70 MJ. This energy is supplied from the storage wall to the air inside the room during periods without sunshine.

Lago and Ismail (2017) presented a convection-conduction model in a square cavity heated on one wall and cooled at the other parallel wall having an internal conducting solid body for a Trombe wall configuration.

In the present study the authors present a numerical model using Volume Finite method and SIMPLE algorithm, which includes heat conduction through the enclosure walls, surface radiation interaction between them and natural convection in the air. The influence of the enclosure wall thickness, emissivity of all surfaces, and thermal conductivity of enclosure wall on flow and heat transfer are analyzed and commented.

2. MATHEMATIC OF MODEL

The problem studied has as a domain a two-dimensional cavity of length L, height H, with aspect ratio H / L = 1, filled with fluid of thermal conductivity k_f and a rectangular solid block of varying thickness and length positioned inside. The upper and lower boundaries of the domain are adiabatic while the left border is defined as constant high temperature, and the right border is defined as constant low temperature. In the interior of the cavity the block will be considered conductor of thermal conductivity k_s. The domain of the problem and the definitions of the boundary conditions used in the work are shown in Fig. 1.

The model is based on the conservation equations of mass, energy and momentum in its two-dimensional and permanent forms. It is assumed that the flow is laminar and incompressible, so the fluid density is considered constant, except for the buoyancy term for which the Boussinesq approximation applies. Field forces acting on the mass of fluid as a whole are admitted as due only to the force of gravity acting in the vertical downward direction. In the energy equation, the viscous dissipation and the compression work are considered negligible. All the thermo-physical properties are considered constant, except for the density in the buoyancy term

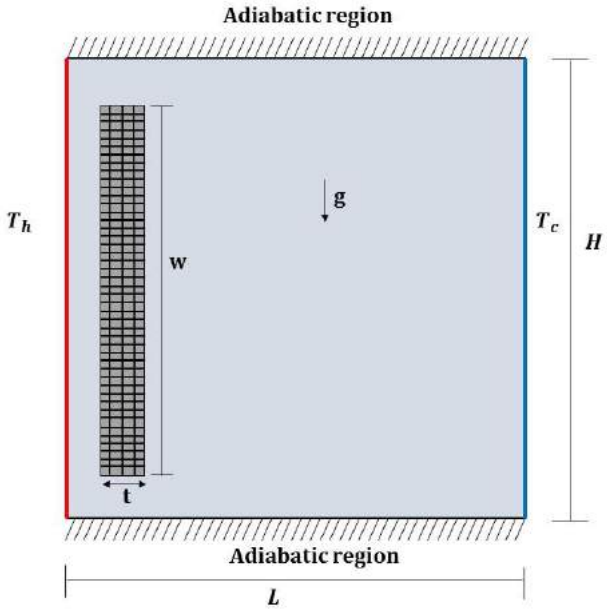

Figure 1. Scheme of the domain of the problem

2.1 Governing Equations

Convective heat transfer can be expressed mathematically by the equation of conservation of mass, the Navier-Stokes equations, and the energy equation. With above-mentioned assumptions, the equations can be written in dimensionless form as follows:

Continuity,

$$\frac{\partial U}{\partial X}+\frac{\partial V}{\partial Y}=0 \tag{1}$$

Momentum,

$$U\frac{\partial U}{\partial X}+V\frac{\partial V}{\partial Y}=-\frac{\partial P}{\partial x}+\Gamma\left(\frac{\partial^2 U}{\partial X^2}+\frac{\partial^2 U}{\partial Y^2}\right) \tag{2}$$

$$U\frac{\partial U}{\partial X}+V\frac{\partial V}{\partial Y}=-\frac{\partial P}{\partial y}+\Gamma\left(\frac{\partial^2 V}{\partial X^2}+\frac{\partial^2 V}{\partial Y^2}\right)+\frac{Ra}{Pr}\theta \tag{3}$$

And Energy,

$$U\frac{\partial \theta}{\partial X}+V\frac{\partial \theta}{\partial Y}=\frac{K}{Pr}\left(\frac{\partial^2 \theta}{\partial X^2}+\frac{\partial^2 \theta}{\partial Y^2}\right) \tag{4}$$

Where Γ is a general diffusion coefficient which is equal to 1 for fluid region and 10^{20} for the region of the solid, and K is a thermal conductivity ratio that is equal to 1 in the region of fluid e $k^* = k_s / k_f$, in solid region.

2.2 Non-dimensional equations

The dimensionless parameters are defined as follows:

$$X=\frac{x}{L},\ Y=\frac{y}{L} \tag{5}$$

$$U=\frac{uL}{\nu},\ V=\frac{\nu L}{\nu} \tag{6}$$

$$P=\frac{p+\rho g y}{\rho\left(\frac{\nu}{L}\right)^2} \tag{7}$$

$$\theta=\frac{T-T_o}{T_h-T_c} \tag{8}$$

$$Ra=\frac{g\beta(T_h-T_c)L^4}{\nu\alpha} \tag{9}$$

$$Pr=\frac{\nu}{\alpha} \tag{10}$$

Here $T_o = (T_h + T_c)/2$ is the reference temperature.

2.3 The boundary conditions

Boundary conditions are stated as follows:

$X = 0 \rightarrow U = V = 0,\ \theta = 0$
$X = 1 \rightarrow U = V = 0,\ \theta = 1$
$Y = 0 \rightarrow U = V = 0,\ \partial\theta/\partial Y + NrQ_r = 0$
$Y = 1 \rightarrow U = V = 0,\ \partial\theta/\partial Y + NrQ_r = 0$

Here $Nr=\sigma\varepsilon T_O H/K(T_H-T_C)$ represents the conduction-radiation number and Q_r represents the dimensionless net radiative heat flux at the insulated walls.

2.4 Radiation between surfaces

In case of all radiation surfaces are grey bodies, the interface radiation heat between liquid and solid is computed by the network method. The effective radiation heat of the ith surface is defined as:

$$Q_{ri} = \varepsilon_i \left[\left(\frac{\theta_i}{\theta_0} + 1 \right)^4 - \sum_{j=1}^{N} F_{ij} (J_j) \right] \tag{11}$$

With,

$$J_i = \varepsilon_i \left(\frac{\theta_i}{\theta_0} + 1 \right)^4 + (1 - \varepsilon_i) \sum_{j=1}^{N} F_{ij} (J_j) \tag{12}$$

Where the summation over the surface element j is to be taken for all the elements of the boundary in which i can interact radiative and $F_{i,j}$ is the differentially view factor, which is calculated using the crossed string method.

2.5 Nusselt Number

To determine the steady state heat transfer characteristics at either of the two vertical walls, contributions of both convection and radiation should be taken into consideration. In the present study the total average Nusselt number is introduced in dimensionless form can be expressed as follows, which is used to calculate Nu at X = 0 and X = 1:

$$Nu = Nu_c + Nu_r = \int_0^1 \frac{\partial \theta}{-\partial X} \partial Y + \int_0^1 Q_r \partial Y \tag{13}$$

3. NUMERICAL PROCEDURE

After establishing the equations that represent the mathematical model and the boundary conditions, the next step is to solve the problem. It is verified that due to the complexity of the equations and boundary conditions, an analytical solution is not feasible and therefore should use numerical resolution techniques. The solution of the dimensionless equations is obtained numerically using the Finite Volume Method in conjunction with the Power-law scheme for discretizing the convective and diffusive energy fluxes. The computational code, written in FORTRAN language, uses SIMPLE algorithm for coupling of pressure and velocity, which is based on a process of velocity field correction based on a pressure field that allows satisfying the mass conservation equation, and the TDMA method in the solution of the systems of equations.

It is convenient to express the conservation equations in their generic form with respect to the conservation of a property φ. For the two-dimensional case in permanent regime, this equation can be written in its conservative form with constant Γφ according to the equation below:

$$\frac{\partial}{\partial x}(\rho u \phi) + \frac{\partial}{\partial x}(\rho v \phi) = \Gamma_\phi \left(\frac{\partial^2 \theta}{\partial x^2} + \frac{\partial^2 \theta}{\partial y^2} \right) + S \tag{14}$$

Where the terms on the left side of the equation correspond to the advective transport of property φ and the first two terms on the right side correspond to the diffusive transport of this property, where Γφ is the diffusive transport coefficient, and the last term of the equation represents a source term. Equation (14) is used to represent the conservation equations from the assignment of specific values for the variables φ, Γ, ρ and S. The representation of the dimensionless equations, for example, is done by assigning the values shown in Tab. 1 to the variables of Eq. (14) for each conservation equation indicated in the table.

Table 1. Values of φ, Γ, ρ and S for conservation equations.

Conservation Principles	ϕ	ρ	Γ	S
Mass	1	1	0	0
Momentum - X	U	1	Flui. = 1 Sol.=10^{20}	$-\frac{\partial P}{\partial Y}$
Momentum - Y	V	1	Flui. = 1 Sol.=10^{20}	$-\frac{\partial P}{\partial Y}+\frac{Ra}{Pr}\theta$
Energy	θ	1	$\frac{K}{Pr}$	NrQ_r

The domain was divided into a uniform grid such that the solid-fluid interface and the domain boundaries coincide with the faces of the control volume. The harmonic mean was used to determine the diffusive coefficients at the interfaces of the control volume (Patankar, 1980). The component velocities were allocated in a staggered grid.

The criterion of convergence used is global convergence. This occurs when mass balance on each control volume and all domains are within a value of 10^{-7} and the residuals for u, v, T and p are about 10^{-7}.

Several numerical tests were done with the purpose of optimizing the computational code, to establish the size of the mesh that does not influence the results and determine the conditions of stability and numerical convergence.

A mesh study was performed for the critical case of Ra = 10^6 and k*=100 with 48x48, 88x88 and 148x148 volumes, with mesh refinement close to solid surfaces. The Nusselt number variation was 0.15% with volumes increasing from 88x88 to 148x148. Hence, the calculations in the present study were obtained for a mesh of 88x88 volumes.

The validation of the problem was performed by comparing the Nusselt number with literature results for cavities with or without the internal solid, showing good agreement. The results for the dimension of solid of the present problem are not available in the literature. In Fig. 2, it is clear that the streamlines of the present solution is very close to De Vahl Davis, 1983 result. These results provide confirmation of the accuracy of the present numerical method to study natural convection in a cavity with partially thermally active side walls.

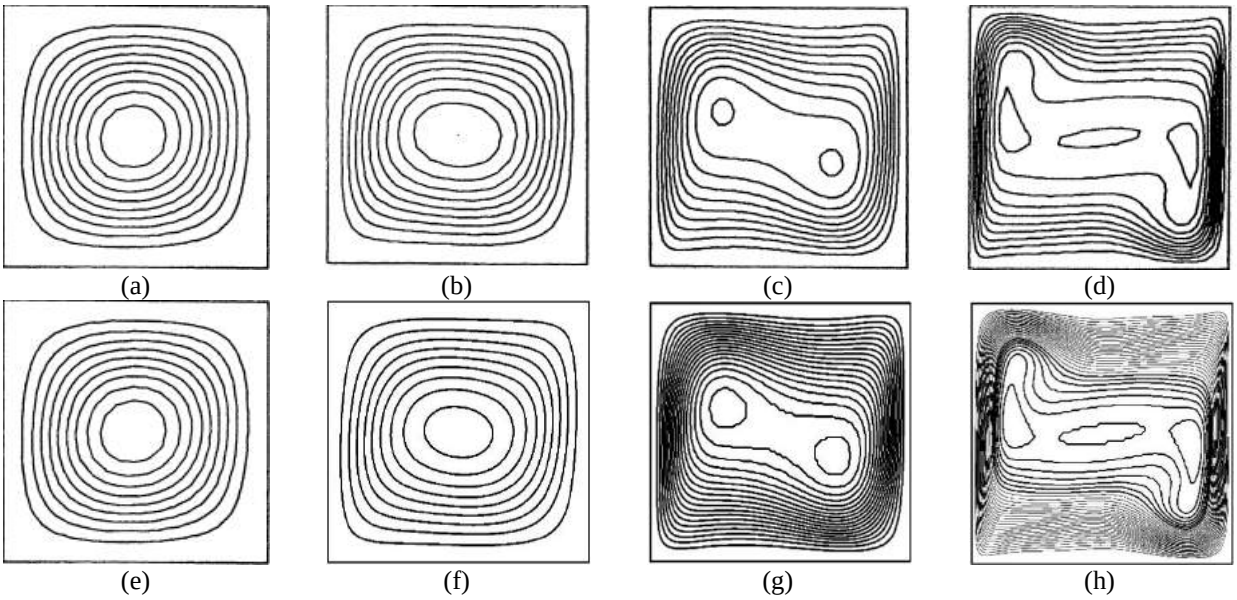

Figure 2. Comparison of the streamlines of the cavity without a body. (a)-(d) Davis results for 10^3,10^4,10^5 and 10^6 (e)-(h) Presents results for 10^3,10^4,10^5 and 10^6

On the other hand, in order to validate the code for cavity with solid, the results were generated and compared with results available in the literature for a cavity heated and cooled from the side with an internal conducting solid of known size (Tab. 2). Table 2 shows the average Nusselt number for a grid of 88x88 control volumes with Pr=0.71. The size of the solid chosen for comparison in the literature occupies the entire central region of the cavity. As can be seen good agreement is obtained indicating that the numerical code predicts satisfactory results for the conjugate heat transfer problem.

Table 2. Comparison of average Nusselt numbers for different Rayleigh numbers.

	$Ra=10^5$, t/L=0.5 and w/H=0.5	
	k*=0.2	k*=5
Present	4.644	4.337
House, *et al*., 1990	4.624	4.324
Zhao, *et al*., 2007	4.660	4.362
Bhave, *et al*., 2006	4.645	4.338
Lima and Ganzarolli (2016)	4.63	4.32

4. PRELIMINARY RESULTS

The preliminary results are given in the form of streamlines and isotherm contour plots. Rayleigh number, temperature ratio (θ_o), emissivity, conductivity ratio are applied as the main effective parameters. The properties of air are mainly set at the reference temperature T_o = 293.5 K. Rayleigh numbers range from 10^3 to 10^6 for keeping the flow regimes under the laminar boundary layer flow. All surfaces of the enclosure are considered to be gray and with the same emissivity which varies from ε = 0, which means there is no radiation heat exchange between the surfaces, to ε = 1.0., which means that surfaces are assumed to be black.

4.1 Effects on Temperature and Flow Field

The general effect of radiation on the isotherms and flow fields can be obtained by setting different emissivities of the surface in the range 0.1-1.0. Figure 3 shows variations of temperature fields with **ε** = 0 and **ε** = 0.5. Surface radiation alters the distribution of the temperature on the insulated walls. The temperature rises at the bottom wall and decreases at the top wall, resulting in the variation of the flow and temperature fields. The temperature gradients near the isothermal walls are relatively weakened, and the thermal boundary layers thickened by surface radiation. Approximate central symmetric contours can also be observed because the smaller temperature difference between the two walls has been given. Streamlines at different ε are shown in Fig. 4, and isotherms are shown in Fig. 5 for Ra = 10^5 The prediction indicates that the appearance of surface radiation can significantly alter the flow and temperature fields even if the given emissivity is quite small, but there are no remarkable changes with the increase of emissivity from 0.1 to 1.0. Surface radiation changes the temperature distribution on the insulated walls, consequently causing variation of the flow and temperature regime. When the steady condition is reached, the distribution of the temperature on the insulated walls mainly depends on the geometrical parameter, the view factor of each subsurface on the insulated walls to those on other surfaces of the enclosure. The increase of emissivity results in greater radiative heat exchange between surfaces.

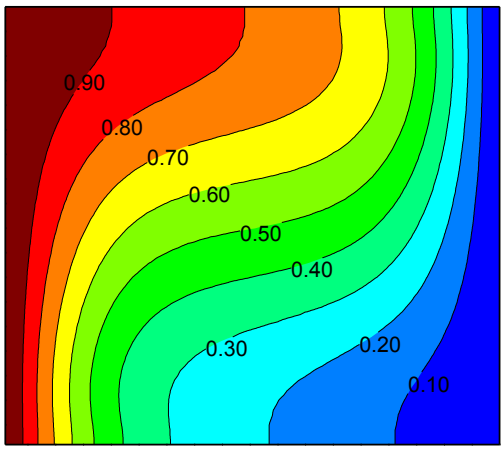

(a)

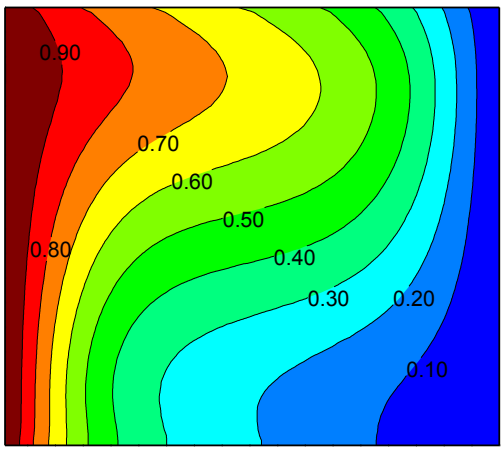

(b)

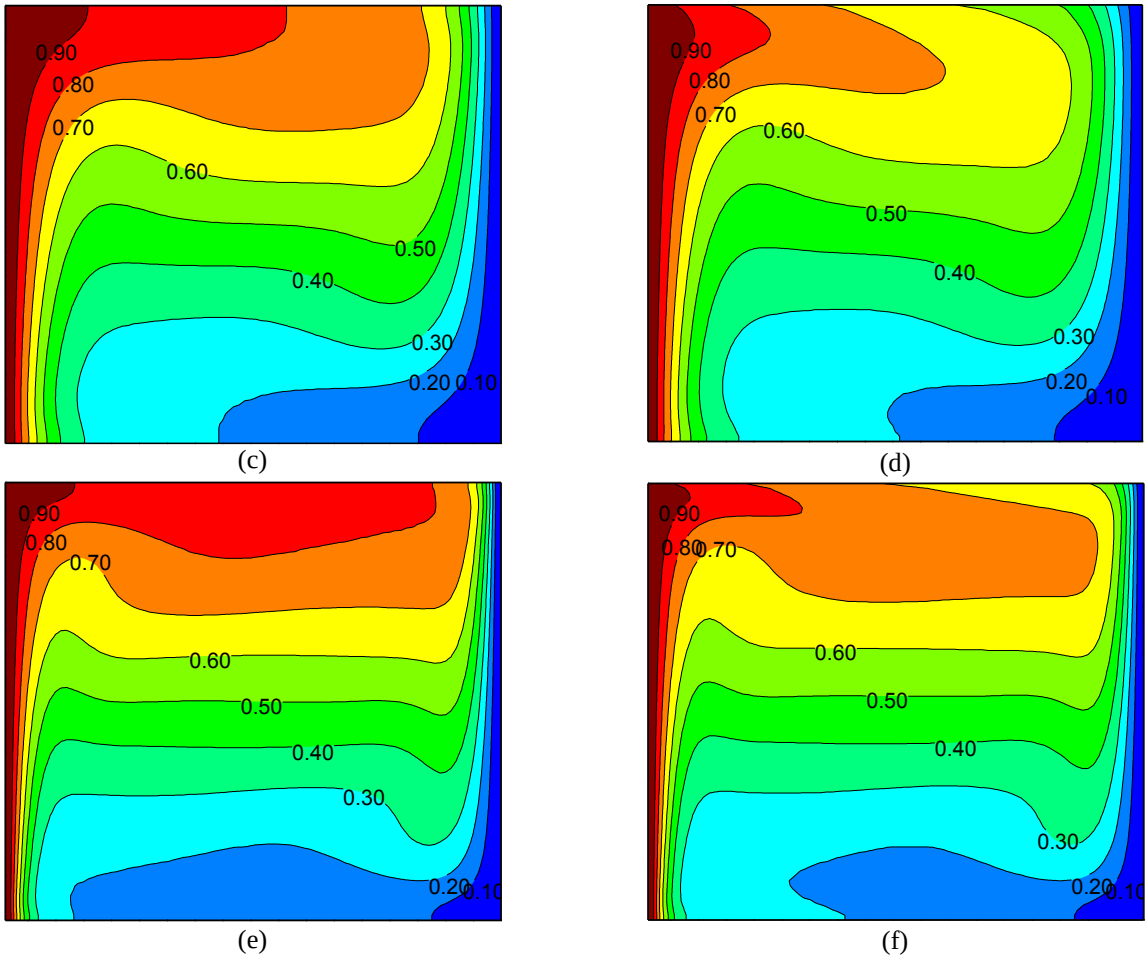

Figure 3. Effect of surface radiation on isotherms. T_o = 293.5 K; Θ_0 = 29.35; Ra = (a)-(b) 10^4, (c)-(d) 10^5, (e)-(f) 10^6); ε= (a)-(c)-(e) 0, (b)-(d)-(f) 0.5.

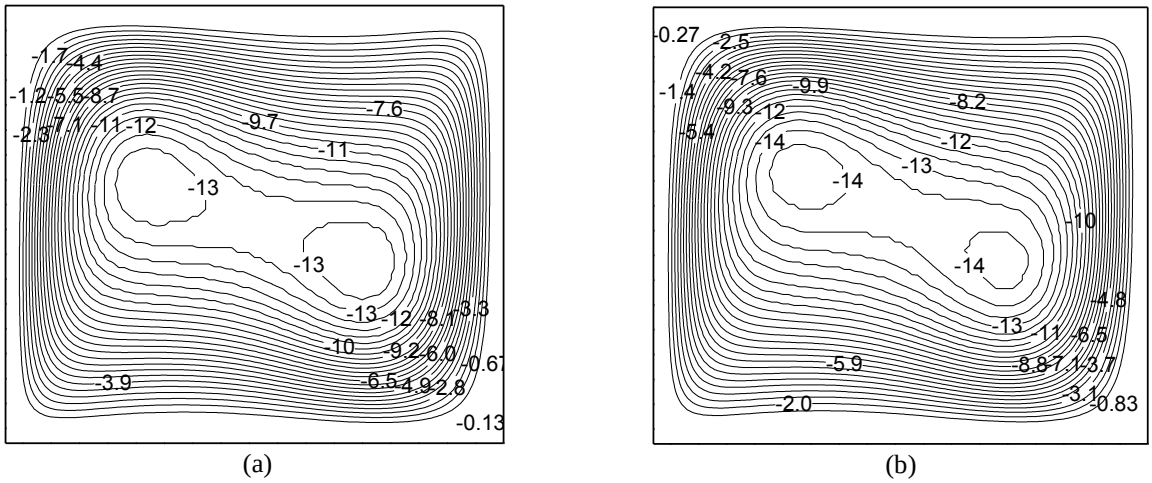

Figure 4. Effect of emissivity on streamlines (T_o = 293.5 K, Ra = 10^5, Θ_0 = 29.35) at (a) ε=0, (b) ε=0.5

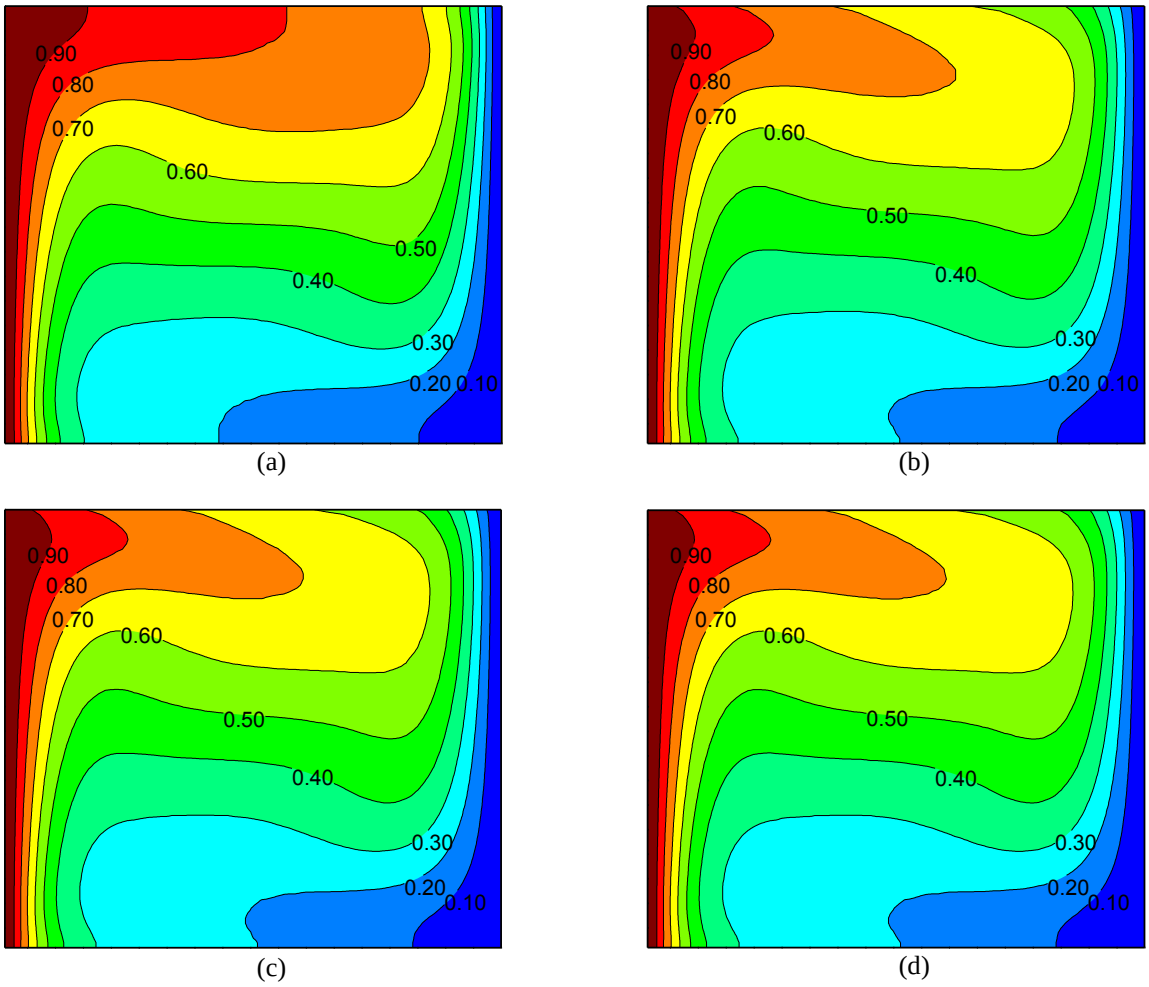

Figure 5. Effect of emissivity on isotherms (T_o = 293.5 K, Ra = 10^5, Θ_0 = 29.35) at (a) ε=0, (b) ε=0.1, (c) ε=0.5, and (d) ε=1.0

The isotherms for the cavity with a conducting body with t/L = 0.2 and w/H=0.9 are shown in Fig. 6 for Ra= 10^6 and ε=0 and 1. The ratios of the thermal conductivity of enclosure wall to the thermal conductivity of air are 1 to 50 for a Rayleigh number of 10^6. When the ratios of the thermal conductivity of enclosure wall to the thermal conductivity of air are different, the temperature fields are greatly different. The influence of the surroundings on inside is intense for k*=50. The temperature in the enclosure is higher than that for k*=5. This is due to the fact that convection is not affected beyond a wall conductivity value above which the wall inner surface temperature becomes almost the same as that of the wall outer surface. In fact, for k*≥ 5, there is only a small temperature gradient in the massive wall. It should be noted that the dimensionless conductivities for various construction materials are usually between 1 and 10, well insulated partitions and walls having k*≈1. The radiation emissivities of all surfaces are 0 and 1 for a Rayleigh number of 10^6. When emissivities of all surfaces are different, the temperature fields are a little different. The influence of emissivity of all surfaces is intense for k*=50. The influence of emissivity of all surfaces is small for k*=1.

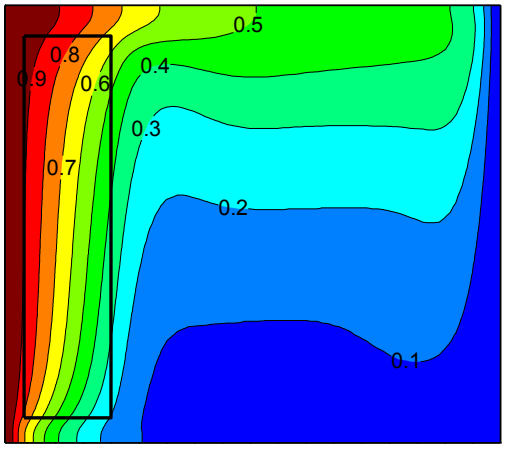
0.9
0.8
0.6
0.5
0.4
0.3
0.7
0.2
0.1

(a)

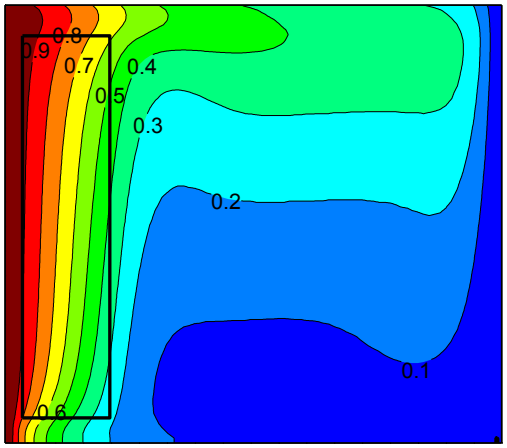
0.9
0.8
0.7
0.4
0.5
0.3
0.2
0.1
0.6

(b)

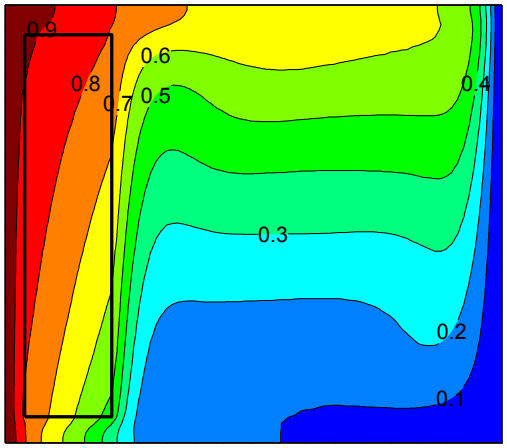
0.9
0.6
0.8
0.7
0.5
0.4
0.3
0.2
0.1

(c)

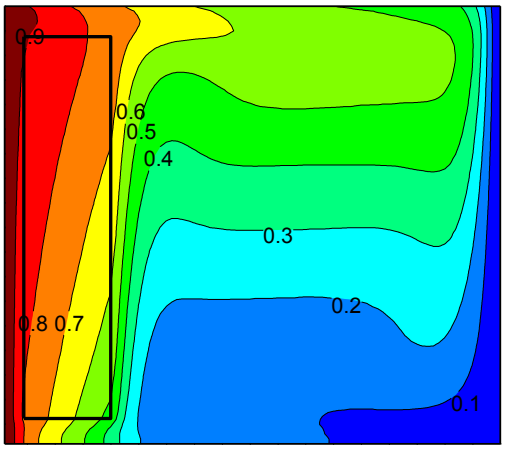
0.9
0.6
0.5
0.4
0.3
0.2
0.8
0.7
0.1

(d)

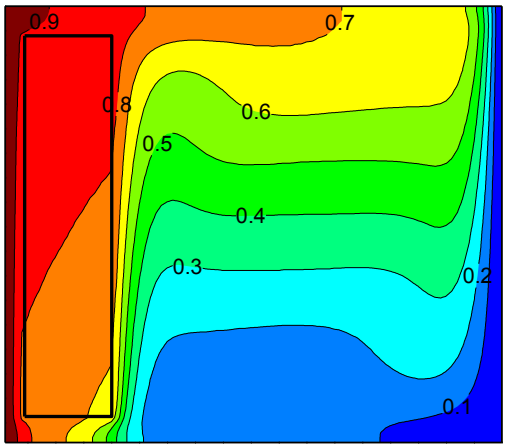
0.9
0.7
0.8
0.6
0.5
0.4
0.3
0.2
0.1

(e)

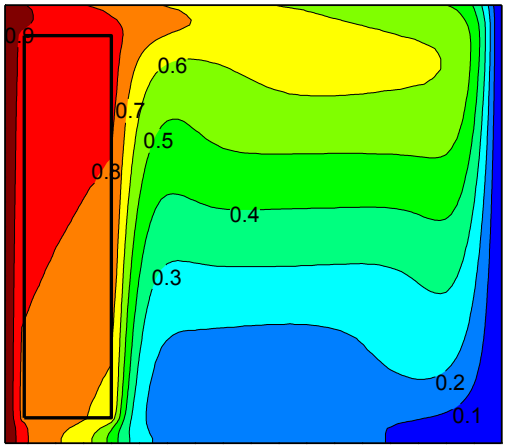
0.9
0.6
0.7
0.5
0.8
0.4
0.3
0.2
0.1

(f)

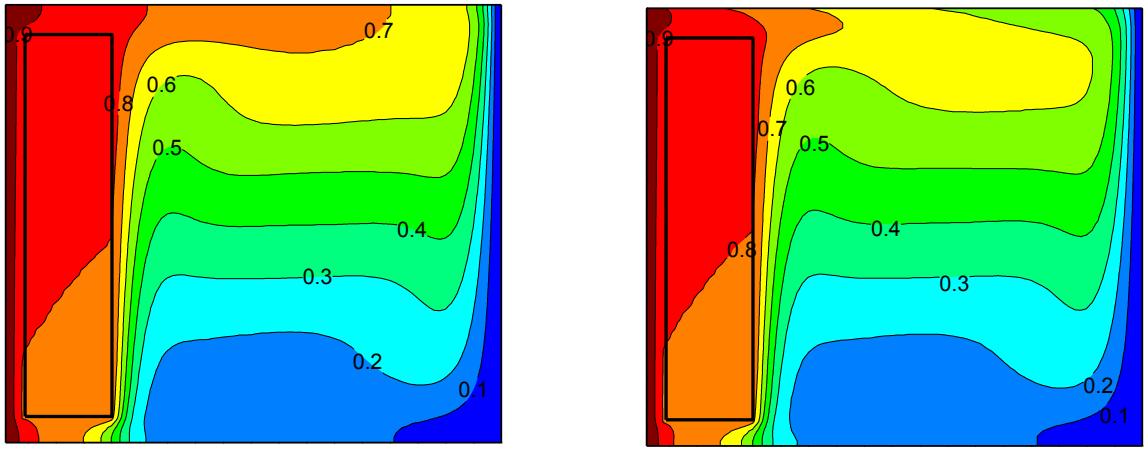

(g) (h)

Figure 6. The temperature fields with solid of t/L = 0.2 and w/H=0.9 (T_o = 293.5 K, Ra = 10^6, Θ_0 = 29.35) at (a) ε=0, k*=1; (b) ε=1, k*=1; (c) ε=0, k*=5; (d) ε=1, k*=5; (e) ε=0, k*=20; (f) ε=1, k*=20; (g) ε=0, k*=50; and (h) ε=1, k*=50

The streamlines are shown in Fig. 7 for a cavity with a long rectangular solid: air is heated in the solid wall, it circulates at the top, and cools down, it circulates again in the bottom of the cavity and below the solid block. As expected, the circulation is stronger as Ra increases, causing narrowing of the stream lines and vortices. The flow in the cavity forms a vortex that rotates clockwise. The profile of the component V presents higher velocity values in the region of the upward flow near the heated wall followed by a region of near uniform descending velocity, and of smaller magnitude, which extends over the rest of the profile. The U component shows higher velocities in the peripheral regions of the profile and smaller velocities in the central region of the cavity.

For Ra = 10^5 and 10^6, the central vortex is pressed between the walls of the cavity and the block generating new rotating cells in the channel and the maximum stream function points of the cavity are shifted towards the formed vortices. The vortices formed when Ra = 10^5 and 10^6 by the isolines of the stream function are located in the central part.

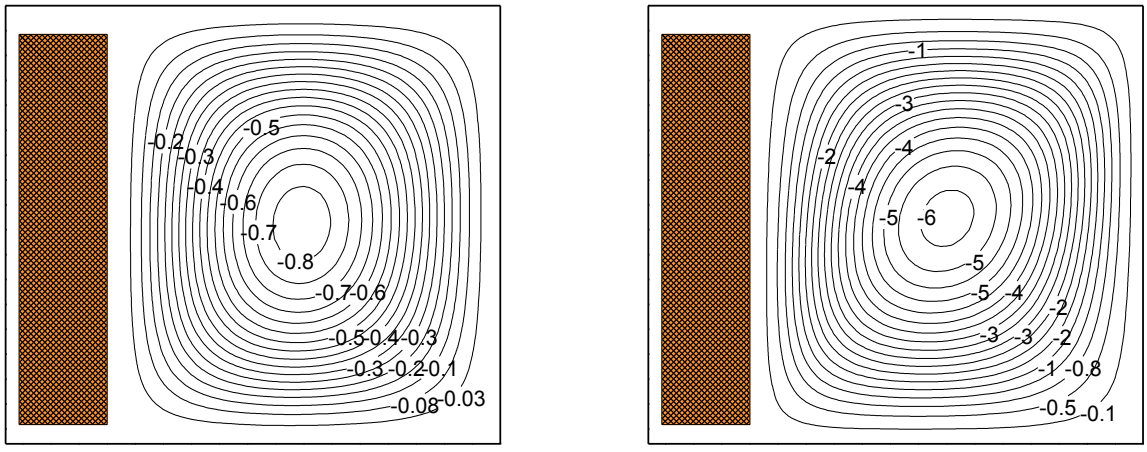

(a) (b)

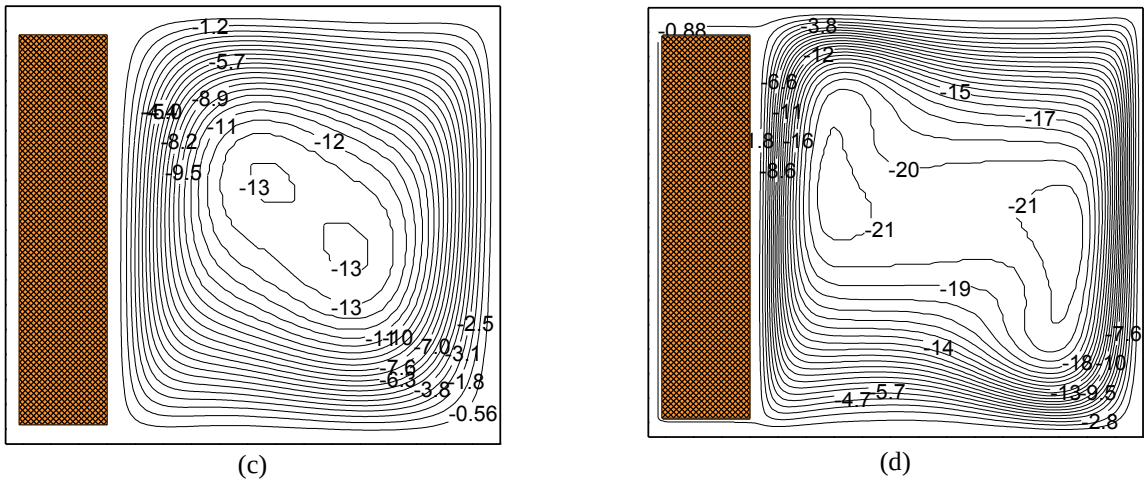

(c) (d)

Figure 7. Streamlines of the cavity with solid of t/L = 0.2 and w/H=0.9 for k*=20, ε=0.7 at (a) Ra =10^3, (b) Ra=10^4, (c) Ra=10^5 and (d) Ra=10^6

4.2 Heat transfer

Heat transfer is evaluated and presented as average Nusselt number of the convection in this section. The dimensionless average Nusselt numbers of convection for t/L = 0.2 and w/H=0.9 and the range of k* (from 0.2 to 50) are respectively shown in Figs. 8 and 9. The effect of wall conductivity on the heat transfer is shown in Fig. 8. It is seen that Nusselt increases in function of k*, weak at low Ra and strong at high Ra with the same trend for different wall thicknesses. This is due to the fact that convection is not affected beyond a wall conductivity above which the wall inner surface temperature becomes almost the same as that of the wall outer surface. In fact, for k*≥ 5, there is only a small temperature gradient in the massive wall. It should be noted that the dimensionless conductivities for various construction materials are usually between 1 and 10, well insulated partitions.

In Fig. 9, the radiation emissivity of all surfaces is from 0 to 1 for a Rayleigh number of 105. With increase of the radiation emissivities of all surfaces, the dimensionless average Nusselt numbers of convection decrease according to linear rule. With decrease of the ratios of the thermal conductivity of enclosure wall to the thermal conductivity of air, the behavior is more obvious. This fact is due to increase radiation emissivities of all surfaces, that become radiation is the dominant way of heat transfer.

For the analysis of the effect of the size of the solid block, the effect of the thickness and the length are investigated. Figs 10 shows the average Nusselt number as function of the dimensionless wall thickness, from 0 to 0.6 for the range of Rayleigh number (from 10^3 to 10^6) for the length of the dimensionless wall chosen.

In Fig. 10, for k *=1 and ε=0.6, it can be seen that with increase of the enclosure wall thicknesses, the dimensionless average Nusselt number of convection decreases. When the cavity wall thickness exceeds 0.2, the increasing speed of dimensionless average Nusselt number of convection decreases. When the cavity wall exceeds certain critical number, the increase of the thickness is invalid for heat transfer.

In Fig. 11 with increase of the solid length, the dimensionless average Nusselt number of convection decreases linearly, for the different Rayleigh numbers as the solid body becomes larger, the flow interference caused by the solid weakens the fluid flow resulting in a decrease in the Nusselt number as observed in Fig.11

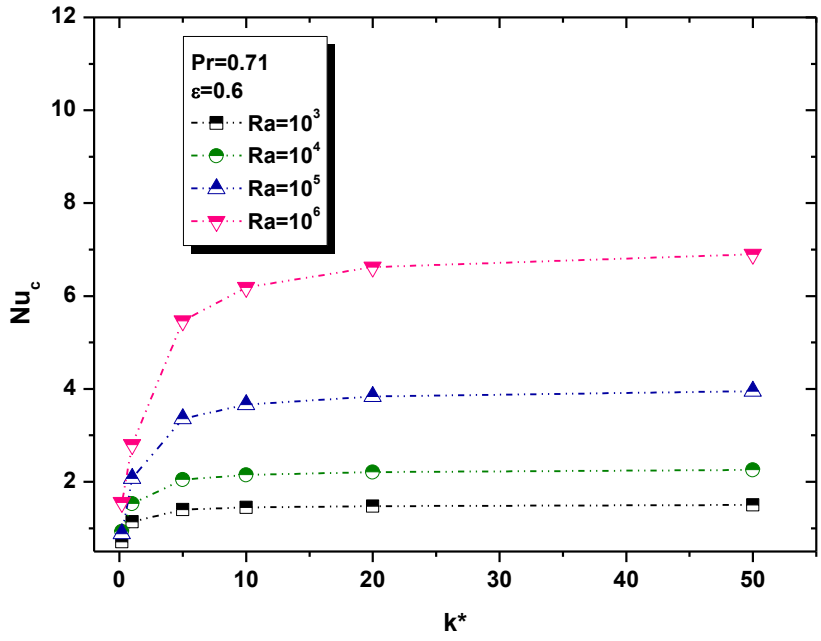

Figure 8. Dimensionless average Nusselt numbers of convection as a function of the wall thermal conductivity for various Rayleigh numbers.

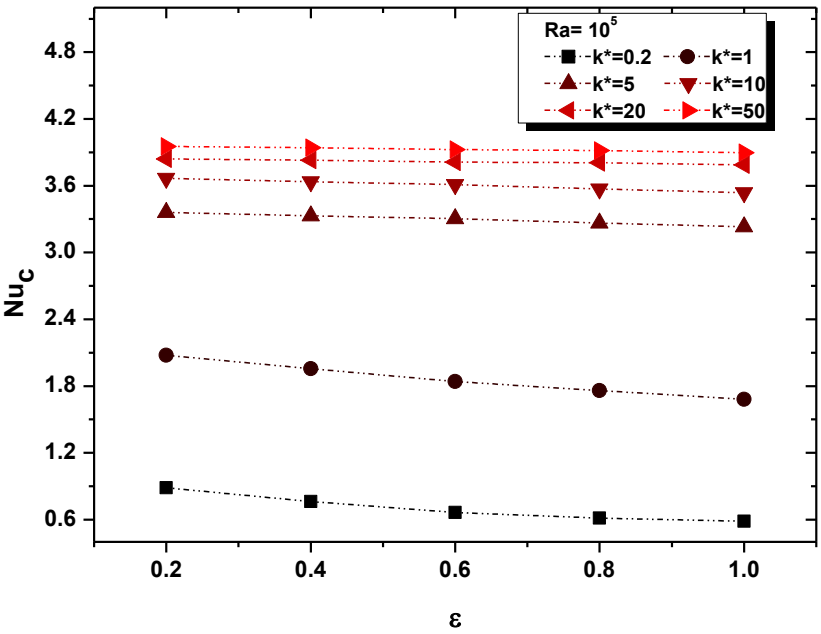

Figure 9. Dimensionless average Nusselt numbers of radiation with increase of the radiation emissivity for $Ra=10^5$.

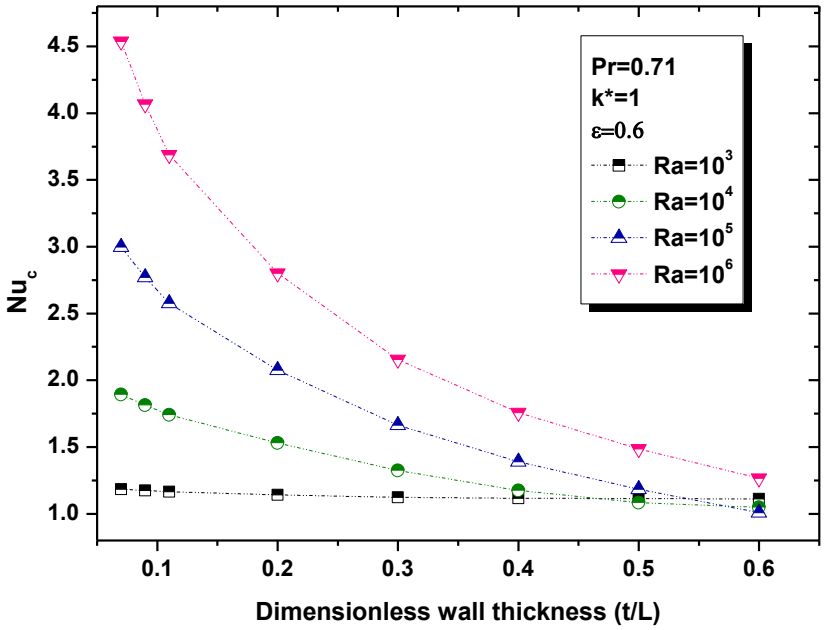

Figure 10. Average Nusselt number for different wall thicknesses and Rayleigh numbers, with k*=1.

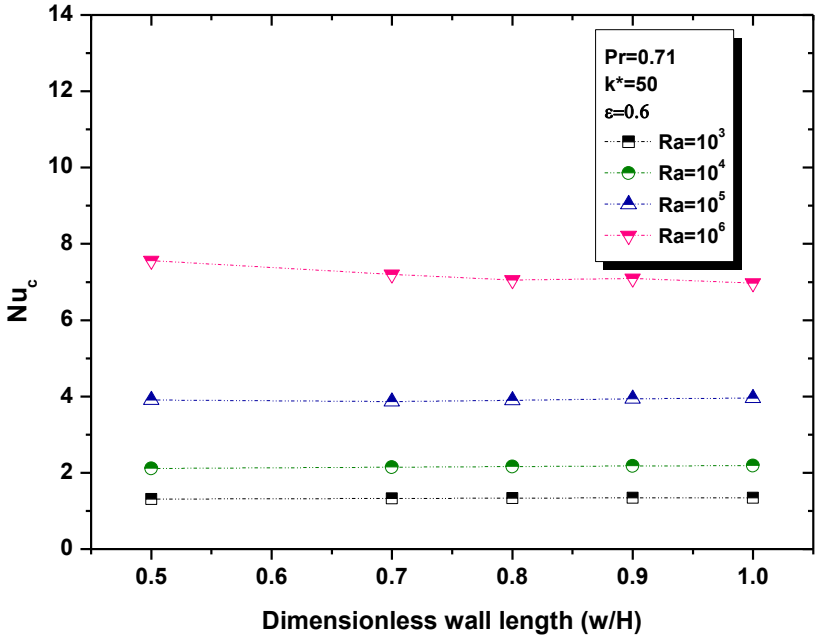

Figure 11. Average Nusselt number for different wall thicknesses and Rayleigh numbers, with k*=50.

5. CONCLUSIONS/ADDITIONS TO THE FINAL PAPER

Numerical investigation using SIMPLE algorithm with Volume finite method for natural convection and heat transfer in the enclosure and radiation coupled in natural convection has been conducted. The results show that flow and heat transfer are influenced by radiation. There are different flows and heat transfer in the enclosure with conduction and radiation. Radiation has a dominant action on flow and heat transfer. With the increase of the thermal conductivity of the enclosure wall, flow and heat transfer become stronger including changes in the temperature distribution. When the thermal conductivity of enclosure wall is more than a certain critical number, the increasing trend of flow and heat transfer

may disappear. When the cavity wall thickness exceeds a certain critical value, the increase of the thickness shows a negligible effect on heat transfer.

6. ACKNOWLEDGEMENTS

The authors would like to acknowledge the doctorate scholar ship for the first author and the PQ research grant for the second author received from the Conselho Nacional de Desenvolvimento Científico e Tecnológico - (CNPq).

7. REFERENCES

Akiyama M. and Chong Q.P., 1997. "Numerical analysis of natural convection with surface radiation in a square enclosure". Numer Heat Transfer, Vol. 32(4), p. 419–433.

Balaji C. and Venkateshan S.P., 1993. "Interaction of surface radiation with free convection in a square cavity". *Int J. Heat Fluid Flow*, Vol. 14, p. 260–267.

Bhave P., Narasimhan A. and Rees DAS, 2006. "Natural convection heat transfer enhancement using adiabatic block: optimal block size and Prandtl number effect". *Int. J. Heat Mass Transfer*, Vol. 49, p. 3807-18.

De Vahl Davis G.,1983. "Natural convection of air in a square cavity: a bench mark numerical solution". *Int. J. Numer. Methods Fluids*, Vol. 3, p. 49-64.

De Vahl Davis G. and Jones, I.P, 1983. "Natural convection in a square cavity: A comparison exercise". *Int J. Numer Method Fluid*, Vol. 3, p. 227–248.

Hernandez-Lopez, I., Xaman, J., Chavez Y., Hernandez-Perez, I. and Alvarado-Juarez, R., 2016. "Thermal energy storage and losses in a room-Trombe wall system located in Mexico". *Sol. Energy*, Vol. 109, p. 512-524.

House J.M., Beckermann C. and Smith T.F., 1990. "Effect of a centered conducting body on natural convection heat transfer in an enclosure". *Numer. Heat Transfer, Part A*, Vol.18, p. 213-22.

Kim D.M. and Viskanta R., 1984. "Effect of wall conduction and radiation on natural convection in a rectangular cavity". Numer Heat Transfer, Vol. 7(4), p. 449–470.

Lago, T.G.S. and Ismail, K.A.R., 2017. "Convection-conduction model for a trombe wall configuration". In *Proceedings of the XXXVIII Iberian Latin-American Congress on Computational Methods in Engineering - CILAMCE2017*. Florianopolis, Brazil.

Lima, T.P. and Ganzarolli, M.M., 2016. "A heat line approach on the analysis of the heat transfer enhancement in a square enclosure with an internal conducting solid body". *Int. Journal of Thermal Sciences*, Vol. 105, p. 45-56.

Mezrhab A., Bouali H., Amaoui H. and Bouzidi M., 2006. "Computation of combined natural convection and radiation heat-transfer in a cavity having a square body at its center". *Appl. Energy*, Vol. 83, p. 1004-23.

Patankar, S.V., 1980. *Numerical Heat Transfer and Fluid Flow*. Hemisphere, New York.

Yedder, R.B. and Bilgen, E., 1991. "Natural convection and conduction in a Trombe wall system". *Int. J. Heat Mass Trans*, Vol. 34, p. 1237-1248.

Zhao, F.Y., Liu D. and Tang, G.F., 2007. "Conjugate heat transfer in square enclosures". *Heat Mass Transfer*, Vol. 43, p. 907-22.

8. RESPONSIBILITY NOTICE

The authors are the only responsible for the printed material included in this paper.